

# THE STRUCTURE AND EVOLUTION OF MOLECULAR CLOUDS: FROM CLUMPS TO CORES TO THE IMF

JONATHAN P. WILLIAMS

*Harvard-Smithsonian Center for Astrophysics*

LEO BLITZ and CHRISTOPHER F. MCKEE

*University of California at Berkeley*

We review the progress that has been made in observing and analyzing molecular cloud structure in recent years. Structures are self-similar over a wide range of scales with similar power law indices independent of the star forming nature of a cloud. Comparison of structures at parsec-scale resolution in a star forming and non-star forming cloud show that the average densities in the former are higher but the structural characteristics in each cloud are much the same. In gravitationally bound regions of a cloud, however, and at higher densities and resolution, the self-similar scaling relationships break down and it is possible to observe the first steps toward star formation. High resolution observations of the dense individual star forming cores within the clumps hold the key to an empirical understanding of the origins of the stellar initial mass function.

## I. INTRODUCTION

Molecular clouds are generally self-gravitating, magnetized, turbulent, compressible fluids. The puzzle of how stars form from molecular clouds begins with understanding the physics of such objects and how individual, gravitationally unstable cores condense within them.

In this review, we describe advances in understanding that have been made since the last *Protostars and Planets* meeting (see the chapter by Blitz in particular, but also chapters by Lada, Strom & Myers, Elmegreen, McKee et al., and Heiles et al.) The predominant point of view at that time was that the inhomogeneous structure that had been observed even in the earliest complete maps of molecular clouds (e.g., Kutner et al. 1977; Blitz & Thaddeus 1980) could be described as a set of discrete clumps (Blitz & Stark 1986). These clumps themselves contain dense cores which are the localized sites of star formation within the cloud (Myers & Benson 1983).

In the intervening years there have been a growing number of papers that describe an alternative point of view: that clouds are scale-

free and their structure is best described as fractal (e.g., Bazell & Désert 1988; Scalo 1990; Falgarone, Phillips, & Walker 1991). In this picture, the hierarchy of cores within clumps within clouds is simply an observational categorization of this self-similar structure. Here we contrast, but also try to reconcile, these two descriptions with a focus on the global questions that link star formation to the ISM: what controls the efficiency and rate of star formation, and what determines the shape of the stellar initial mass function (IMF)?

We begin by describing the large scale view of the molecular ISM, and move to progressively smaller scales. The study of molecular clouds is a broad topic and to stay close to the title of this meeting, we concentrate on the structure and evolution of the star forming regions in these clouds.

## II. THE LARGE SCALE VIEW

Advances in millimeter-wave receiver technology have made it possible to map molecular clouds rapidly at high sensitivity. The noise in an observation is directly proportional to the system temperature, and as receiver temperatures have decreased, it has become feasible to map entire complexes – degrees in angular size – at sub-arcminute resolution. Focal plane arrays (arrays of receivers observing neighboring points of the sky simultaneously) at the FCRAO 14 m and NRAO 12 m single dish telescopes have increased the mapping speed by an order of magnitude. Up to four receivers operating at different frequencies can be used simultaneously at the IRAM 30 m telescope to observe the same position on the sky. The expansion of the millimeter-wave interferometers, IRAM, OVRO, and BIMA has dramatically increased the imaging quality and sensitivity of these instruments and has made high resolution observations ( $< 10''$ ) of structure in molecular clouds considerably quicker and easier.

Most of the mass of the molecular ISM is in the form of giant molecular clouds (GMCs), with masses  $\sim 10^{5-6} M_{\odot}$ , diameters  $\sim 50$  pc, and average densities,  $\langle n_{\text{H}_2} \rangle \sim 10^2 \text{ cm}^{-3}$  (e.g., Blitz 1993). The sharp cut-off at the upper end of the cloud mass distribution at  $\sim 6 \times 10^6 M_{\odot}$  (Williams & McKee 1997) indicates that cloud masses are limited by some physical process, such as the tidal field of the Galaxy or the disrupting effect of massive stars within them.

The FCRAO telescope has recently completed a sensitive, high resolution, unbiased study of the CO emission in the outer Galaxy (Heyer et al. 1998). There is no distance ambiguity in the outer Galaxy and much less blending of emission, and therefore this survey allows a more detailed investigation of the large scale structure of the ISM (see Figure 1) than earlier surveys of the inner Galaxy by Dame et al. (1987) and Sanders et al. (1985). Heyer et al. (1998) confirm that

there are large regions with little or no CO emission (Dame et al. 1986) and concur with earlier results that these regions have been cleared of molecular gas by the intense radiation fields and stellar winds from massive stars. Further recent observations of the structural imprint of massive star formation in individual star forming regions is discussed by Patel et al. (1995), Carpenter, Snell, & Shloerb (1995a), and Heyer, Carpenter, & Ladd (1996). Carpenter, Snell, & Shloerb (1995b) suggest that massive stars can act to compress gas and create dense cores that give rise to the next generation of star formation as originally proposed by Elmegreen & Lada (1977).

Heyer & Terebey (1998) and Digel et al. (1996) show that CO emission in the outer Galaxy is confined almost exclusively to the spiral arms, confirming the earlier results of Cohen et al. (1980). The former, most recent work shows that the ratio of emission in the arm to interarm regions is greater than 28:1. The absence of molecular gas in the interarm regions implies that molecular clouds form from a compressed atomic medium, and have lifetimes that are less than an arm crossing time  $\sim 10^7$  yr. These conclusions may not apply in the inner Galaxy where it has been more difficult to isolate arm emission and calculate an arm-to-interarm ratio. Solomon & Rivolo (1989) have argued that about half the CO in the inner Galaxy is in clouds that are not actively forming stars, and that this gas is not concentrated in spiral arms. However, Loinard et al. (1996) find an arm-to-interarm ratio  $\sim 10 : 1$  in M31 in the south-west “ring”  $\sim 9$  kpc from the galaxy center which suggests that similar conclusions about cloud formation and lifetimes can be drawn in that galaxy too.

There have been several recent studies of HI halos around molecular clouds (e.g. Kuchar & Bania 1993; Williams & Maddalena 1996; Moriarty-Schieven, Andersson & Wannier 1997) and a comprehensive survey is underway at the DRAO telescope (Normandeau, Taylor, & Dewdney 1997). In order to form a GMC of mass  $10^6 M_{\odot}$  out of an atomic ISM of density  $\langle n_{\text{H}} \rangle \sim 1 \text{ cm}^{-3}$ , gas must be accumulated from a volume  $\sim 0.4$  kpc in diameter. Since such a large region encompasses many atomic clouds, the density inhomogeneities in molecular clouds may simply reflect the initial non-uniform conditions of their formation rather than the first step in the fragmentation/condensation process that leads to the creation of stars (Elmegreen 1985). To distinguish between the remnants of the formation of a cloud and the first steps toward star formation, it is necessary to analyze and compare structures in a number of different clouds.

### III. CLOUD STRUCTURE AND SELF-SIMILARITY

#### A. A categorization of molecular cloud structure

Before we discuss the analysis of cloud structure, we first define an operational categorization into clouds, clumps, and cores. This categorization is not inconsistent with the fractal models for cloud structure that are discussed in §III.E, although we argue that gravity introduces scales that limit the range of validity of the fractal description.

Molecular clouds are regions in which the gas is primarily molecular. Almost all known molecular clouds in the Galaxy are detectable in CO. Giant molecular clouds have masses  $\gtrsim 10^4 M_\odot$ , are generally gravitationally bound, and may contain several sites of star formation. However, there also exist small molecular clouds with masses  $\lesssim 10^2 M_\odot$ , such as the unbound high latitude clouds discovered by Blitz, Magnani, & Mundy (1984), and the small, gravitationally bound molecular clouds in the Galactic plane cataloged by Clemens & Barvainis (1988). A small number of low mass stars are observed to form in some of these clouds but the contribution to their total star formation rate in the Galaxy is negligible (Magnani et al. 1995).

Clumps are coherent regions in  $l-b-v$  space, generally identified from spectral line maps of molecular emission. Star-forming clumps are the massive clumps out of which stellar clusters form. Although most clusters are unbound, the gas out of which they form is bound (Williams, Blitz, & Stark 1995). Cores are regions out of which single stars (or multiple systems such as binaries) form and are necessarily gravitationally bound. Not all material that goes into forming a star must come from the core; some may be accreted from the surrounding clump or cloud as the protostar moves through it (Bonnell et al. 1997).

We have discussed this categorization to describe observations in a uniform manner and to provide a clear link to the processes of star formation. In the following sections we adopt this classification and discuss the relationship between the structure of molecular clouds and their evolution toward star formation.

#### B. The virial theorem for molecular clouds

The condition for a molecular cloud or clump within it to be gravitationally bound can be inferred from the virial theorem, which may be written

$$\frac{1}{2}\ddot{I} = 2(\mathcal{T} - \mathcal{T}_0) + \mathcal{M} + \mathcal{W}, \quad (1)$$

where  $I$  is the moment of inertia,  $\mathcal{T}$  is the total kinetic energy (including thermal),  $\mathcal{M}$  is the net magnetic energy, and  $\mathcal{W}$  is the gravitational energy (see McKee et al. 1993 for more details). The moment of inertia term is usually neglected, but it may be significant for a turbulent cloud.

In contrast to the terms on the RHS of the equation, it can be of either sign, and as a result its effects can be averaged out either by applying the virial theorem to an ensemble of clouds or clumps or by averaging over a time long compared with the dynamical time (assuming the cloud lives that long.) The kinetic energy term,

$$\mathcal{T} = \int_{V_{\text{cl}}} \left( \frac{3}{2} P_{\text{th}} + \frac{1}{2} \rho v^2 \right) dV \equiv \frac{3}{2} \bar{P} V_{\text{cl}}, \quad (2)$$

includes both the thermal and non-thermal pressure inside the cloud. The surface term can be expressed as  $\mathcal{T}_0 = \frac{3}{2} P_0 V_{\text{cl}}$ , where  $P_0$  is about equal to the total thermal plus nonthermal pressure in the ambient medium (McKee and Zweibel 1992). Finally, the gravitational term can be written as (Bertoldi and McKee 1992)

$$\mathcal{W} \equiv -3P_G V_{\text{cl}}, \quad (3)$$

where the “gravitational pressure”  $P_G$  is the mean weight of the material in the cloud. With these results, the steady-state, or time-averaged, virial theorem becomes

$$\bar{P} = P_0 + P_G \left( 1 - \frac{\mathcal{M}}{|\mathcal{W}|} \right). \quad (4)$$

In this form, the virial theorem has an immediate intuitive meaning: the mean pressure inside the cloud is the surface pressure plus the weight of the material inside the cloud, reduced by the magnetic stresses.

In the absence of an external gravitational field,  $\mathcal{W}$  is the gravitational energy of the cloud,

$$\mathcal{W} = -\frac{3}{5} a \left( \frac{GM^2}{R} \right), \quad (5)$$

where  $a$  is a numerical factor of order unity that has been evaluated by Bertoldi and McKee (1992). The gravitational pressure is then

$$P_G = \left( \frac{3\pi a}{20} \right) G \Sigma^2 \rightarrow 5540 \bar{A}_V^2 \text{ K cm}^{-3}, \quad (6)$$

where  $\Sigma$  is the mean surface density of the cloud and  $\bar{A}_V$  is the corresponding visual extinction. The numerical evaluation is for a spherical cloud with a  $1/r$  density profile.

Magnetic fields play a crucial role in the structure and evolution of molecular clouds. For poloidal fields, the relative importance of gravity and magnetic field is determined by the ratio of the mass to the *magnetic critical mass*,

$$M_\Phi = \frac{c_\Phi \Phi}{G^{1/2}}. \quad (7)$$

The value of the numerical factor  $c_\Phi$  depends on the distribution of mass to flux. If the mass-to-flux ratio is constant, then  $c_\Phi = 1/2\pi$  (Nakano & Nakamura 1978). In this case, the ratio of the magnetic force to the gravitational force is (in our notation)  $(M_\Phi/M)^2$  (Shu & Li 1997), which is invariant so long as the magnetic flux is frozen to the matter. For  $M < M_\Phi$ , the cloud is said to be *magnetically subcritical*: such a cloud can never undergo gravitational collapse (so long as flux freezing holds) since the magnetic force always exceeds the gravitational force. Conversely, if  $M > M_\Phi$ , the cloud is *magnetically supercritical*, and magnetic fields cannot prevent gravitational collapse. Shu & Li (1997) have presented a general analysis of the forces in magnetized disks with a constant mass-to-flux ratio (which they term “isopedic” disks); their analysis applies even if the disks are non-axisymmetric and time-dependent. The distinction between magnetically subcritical and supercritical disks holds for non-isopedic disks as well, although the value of  $c_\Phi$  may differ; for example, for a mass-to-flux distribution corresponding to a uniform field threading a uniform, spherical cloud, Tomisaka et al. (1988) find  $c_\Phi \simeq 0.12$ .

Toroidal fields can provide a confining force, thereby reducing the magnetic critical mass (Tomisaka 1991; Fiege & Pudritz 1998). However, the ratio of the toroidal field to the poloidal field cannot become too large without engendering instabilities (e.g., Jackson 1975).

If the cloud is supported by thermal and nonthermal pressure in addition to the magnetic stresses, then the maximum stable mass is the critical mass  $M_{\text{cr}}$ , and the cloud is subcritical for  $M < M_{\text{cr}}$  and supercritical for  $M > M_{\text{cr}}$ . For an isothermal cloud, the critical mass is given by  $M_{\text{cr}} \simeq M_\Phi + M_{\text{BE}}$ , where the Bonnor-Ebert mass  $M_{\text{BE}} = 1.18c_s^4/(G^3P_0)^{1/2}$  is the largest gravitationally stable mass at an exterior pressure  $P_0$  for a nonmagnetic sphere (McKee 1989).

What do observations say about the importance of magnetic fields in clouds? The most detailed study is that of the cloud B1, for which Crutcher et al. (1994) found that the inner envelope was marginally magnetically subcritical, whereas the densest region was somewhat supercritical. The observational results were shown to be in good agreement with a numerical model that, however, did not include the observed nonthermal motions. Crutcher (1999) has summarized the observations of magnetic fields in a number of clouds, and finds that they are magnetically supercritical; in this sample, which tends to focus on the central regions of clouds, there is no clear case in which a cloud is magnetically subcritical. If the magnetic field makes an angle  $\theta$  with respect to the line of sight, then the observed field is smaller than the true value by a factor  $\cos\theta$ ; on average, this is a factor 1/2. After allowing for this, he finds that on average  $\langle M/M_\Phi \rangle \simeq 2.5$ . If the clouds are flattened along the field lines, then the observed area is smaller than the true area by factor  $\cos\theta$  as well, so that  $M/M_\Phi \propto \cos^2\theta$ ; on average,

this is a factor 1/3. However, since clouds are observed to have substantial motions, they are unlikely to be highly flattened along field lines, so Crutcher concludes that  $\langle M/M_\Phi \rangle \simeq 2$ . The idea that GMCs are magnetically supercritical with  $M/M_\Phi \simeq 2$  was suggested theoretically by McKee (1989); Bertoldi & McKee (1992) extended this argument to star forming clumps, and Nakano (1998) argued that cores are magnetically supercritical. Crutcher (1999) also finds that the Alfvén Mach number of the motions,  $m_A = \sigma\sqrt{3}/v_A$ , is about unity, as inferred previously by others on the basis of less complete data (e.g., Myers & Goodman 1988).

With these results in hand, we can now address the issue of whether molecular clouds and their constituents are gravitationally bound. The virial theorem (eq. 4) enables us to write the total energy  $E = \mathcal{T} + \mathcal{M} + \mathcal{W}$  as

$$E = \frac{3}{2} \left[ P_0 - P_G \left( 1 - \frac{\mathcal{M}}{|\mathcal{W}|} \right) \right] V_{\text{cl}}. \quad (8)$$

In the absence of a magnetic field, the condition that the cloud be bound (i.e.,  $E < 0$ ) is simply  $P_G > P_0$ . We shall use this criterion even for magnetized clouds, bearing in mind that using the total ambient gas pressure for  $P_0$  is an overestimate and that our analysis is approximate because we have used the time-averaged virial theorem.

For GMCs, the surface pressure is that of the ambient interstellar medium. In the solar vicinity, the total interstellar pressure, which balances the weight of the ISM, is about  $2.8 \times 10^4 \text{ K cm}^{-3}$  (Boulares and Cox 1990). Of this, about  $0.7 \times 10^4 \text{ K cm}^{-3}$  is due to cosmic rays; since they pervade both the ISM and a molecular cloud, they do not contribute to the support of a cloud and may be neglected. The magnetic pressure is about  $0.3 \times 10^4 \text{ K cm}^{-3}$  (Heiles 1996), leaving  $P_0 \simeq 1.8 \times 10^4 \text{ K cm}^{-3}$  as the total ambient gas pressure.

What is the minimum value of  $P_G$  for a molecular cloud? According to van Dishoeck and Black (1988), molecular clouds exposed to the local interstellar radiation field have a layer of  $\text{C}^+$  and  $\text{C}^0$  corresponding to a visual extinction of 0.7 mag. If we require at least 1/3 of the carbon along a line of sight through a cloud to be in the form of CO in order for it to be considered “molecular”, then the total visual extinction must be  $A_V > 2$  mag (allowing for a shielding layer on both sides). According to equation (6), this gives  $P_G \gtrsim 2 \times 10^4 \text{ K cm}^{-3} \sim P_0$ , verifying that molecular clouds as observed in CO are at least marginally bound (e.g. Larson 1981). Note that if we defined molecular clouds as having a significant fraction of  $\text{H}_2$  rather than CO, the minimum column density required would be substantially less and the clouds might not be bound. Furthermore, the conclusion that CO clouds are bound depends both on the interstellar pressure and on the strength of the FUV radiation field, and CO clouds may not be bound everywhere in the Galaxy or

in other galaxies (Elmegreen 1993b).

GMCs in the solar neighborhood typically have mean extinctions significantly greater than 2 mag, and as a result  $P_G$  is generally significantly greater than  $P_0$ . For GMCs in the solar neighborhood,  $P_G \sim 2 \times 10^5 \text{ K cm}^{-3}$ , an order of magnitude greater than  $P_0$  (Blitz 1991; Bertoldi & McKee 1992; Williams et al. 1995). Thus if GMCs are dynamically stable entities (the crossing time for a GMC is about  $10^7$  y, smaller than the expected lifetime – see Blitz & Shu 1980), then GMCs must be self-gravitating. In the inner galaxy, where  $P_0$  is expected to be greater, the typical GMC linewidths also appear to be somewhat greater than those found locally (Sanders, Scoville, & Solomon 1985), and thus  $P_G$  is still comfortably greater than  $P_0$ .

For clumps within GMCs, the surface pressure is just the mean pressure inside the GMC,  $P_G(\text{GMC}) \propto \Sigma^2(\text{GMC})$ , so the virial theorem becomes  $\bar{P}(\text{clump}) \propto \Sigma^2(\text{GMC}) + \Sigma^2(\text{clump})$ . Most clumps observed in  $^{13}\text{CO}$  have  $\Sigma(\text{clump}) \ll \Sigma(\text{GMC})$  and are therefore confined by pressure rather than gravity; on the other hand, much of the mass is in massive star-forming clumps that have  $\Sigma(\text{clump}) \gtrsim \Sigma(\text{GMC})$  and are therefore gravitationally bound (Bertoldi and McKee 1992).

### C. Structure analysis techniques

Molecular cloud structure can be mapped via radio spectroscopy of molecular lines (e.g., Bally et al. 1987), continuum emission from dust (e.g., Wood, Myers, & Daugherty 1994), or stellar absorption by dust (Lada et al. 1994). The first gives kinematical as well as spatial information and results in a three dimensional cube of data, whereas the latter two result in two dimensional datasets. Many different techniques have been developed to analyze these data which we discuss briefly here.

Stutzki & Güsten (1990) and Williams, de Geus, & Blitz (1994) use the most direct approach and decompose the data into a set of discrete clumps, the first based on recursive tri-axial gaussian fits, and the latter by identifying peaks of emission and then tracing contours to lower levels. The resulting clumps can be considered to be the “building blocks” of the cloud and may be analyzed in any number of ways to determine a size-linewidth relation, mass spectrum, and variations in cloud conditions as a function of position (Williams et al. 1995). There are caveats associated with each method of clump deconvolution, however. Since the structures in a spectral line map of a molecular cloud are not, in general, gaussian, the recursive fitting method of Stutzki & Güsten (1990) will tend to find and subsequently fit residuals around each clump, which results in a mass spectrum that is steeper than the true distribution. On the other hand, the contour tracing method of Williams et al. (1994) has a tendency to blend small features with larger structures and results in a mass spectrum that is flatter than the true distribution.



Heyer & Schloerb (1997) use principal component analysis to identify differences in line profiles over a map. A series of eigenvectors and eigenimages are created which identify ever smaller velocity fluctuations and their spatial distribution, resulting in the determination of a size-linewidth relation. Langer, Wilson, & Anderson (1993) use Laplacian pyramid transforms (a generalization of the Fourier transform) to measure the power on different size scales in a map; as an application, they determine the mass spectrum in the B5 molecular cloud. Recently, Stutzki et al. (1998) have described a closely related Allan-variance technique to characterize the fractal structure of 2-dimensional maps. Houlahan & Scalo (1992) define an algorithm that constructs a structure tree for a map; this retains the spatial relation of the individual components within the map but loses information regarding their shapes and sizes. It is most useful for displaying and ordering the hierarchical nature of the structures in a cloud.

Adams (1992) discusses a topological approach to quantify the difference between maps. Various “output functions” (e.g., distribution of density, volume, and number of components as a function of column density; see Wiseman & Adams 1994) are calculated for each cloud dataset and a suitably defined metric is used to determine the distance between these functions and therefore to quantify how similar clouds are, or to rank a set of clouds.

A completely different technique was pioneered by Lada et al. (1994). They determine a dust column density in the dark cloud IC 5146 by star counts in the near-infrared and mapped cloud structure over a much greater dynamic range ( $A_V = 0 - 32$  mag) than a single spectral line map.

The most striking result of applying these various analysis tools to molecular cloud datasets is the identification of self-similar structures characterized by power law relationships between, most famously, the size and linewidth of features (Larson 1981), and the number of objects of a given mass (e.g., Loren 1989). Indeed, mass spectra are observed to follow a power law with nearly the same exponent,  $x = 0.6 - 0.8$ , where  $dN/d \ln M \propto M^{-x}$  from clouds with masses up to  $10^5 M_\odot$  in the outer Galaxy to features in nearby high-latitude clouds with masses as small as  $10^{-4} M_\odot$  (Heyer & Terebey 1998; Kramer et al. 1998a; Heithausen et al. 1998). Since a power law does not have a characteristic scale, the implication is that clouds and their internal structure are scale-free. This is a powerful motivation for a fractal description of the molecular ISM (Falgarone et al. 1991, Elmegreen 1997a). On the other hand, molecular cloud maps do have clearly identifiable features, especially in spectral line maps when a velocity axis can be used to separate kinematically distinct features along a line of sight (Blitz 1993). These features are commonly called clumps, but there are also filaments (e.g., Nagahama et al. 1998), and rings, cavities, and shells (e.g., Carpenter

et al. 1995a).

#### D. Clumps

Clump decomposition methods such as those described above by Stutzki & Güsten (1990) and Williams et al. (1994) can be readily visualized and have an appealing simplicity. In addition, as for all automated techniques, these algorithms offer an unbiased way to analyze datasets, and are still a valid and useful tool for cloud comparisons even if one does not subscribe to the notion of clumps within clouds as a physical reality (Scalo 1990).

In a comparative study of two clouds, Williams et al. (1994) searched for differences in cloud structure between a star forming and non-star forming GMC. The datasets they analyzed were maps of  $^{13}\text{CO}(1-0)$  emission with similar spatial (0.7 pc) and velocity resolution ( $0.68 \text{ km s}^{-1}$ ) but the two clouds, although of similar mass  $\sim 10^5 M_{\odot}$ , have very different levels of star formation activity. The first, the Rosette molecular cloud, is associated with an HII region powered by a cluster of 17 O and B stars and also contains a number of bright infrared sources from ongoing star formation deeper within the cloud (Cox, Deharveng, & Leene 1990). The second cloud, G216-2.5, originally discovered by Maddalena & Thaddeus (1985), contains no IRAS sources from sites of embedded star formation and has an exceptionally low far-infrared luminosity to mass ratio (Blitz 1990),  $L_{\text{IR}}/M_{\text{cloud}} < 0.07 L_{\odot}/M_{\odot}$ , compared to more typical values of order unity (see Williams & Blitz 1998).

Almost 100 clumps were cataloged in each cloud, and sizes, linewidths, and masses were calculated for each. These basic quantities were found to be related by power laws with the same index for the two clouds, but with different offsets (Figure 2) in the sense that for a given mass, clumps in the non-star forming cloud are larger, and have greater linewidths than in the star forming cloud. The similarity of the power law indices suggests that, on these scales,  $\sim$  few pc, and at the low average densities,  $\langle n_{\text{H}_2} \rangle \sim 300 \text{ cm}^{-3}$ , of the observed clumps, the principal difference between the star forming and non-star forming cloud is the change of scale rather than the collective nature of the structures in each cloud.

Figure 2 shows that the kinetic energy of each clump in G216-2.5 exceeds its gravitational potential energy, and therefore no clump in the cloud is bound (although the cloud as a whole is bound). On the other hand, Williams et al. (1995) show that, for the Rosette molecular cloud, stars formation occurs only in the gravitationally bound clumps in the cloud. Therefore, the lack of bound clumps in G216-2.5 may explain why there is no star formation currently taking place within it.

Even in the Rosette cloud, most clumps are not gravitationally bound. These unbound clumps have similar density profiles,  $n(r) \propto$

$1/r^2$ , as the bound clumps (Williams et al. 1995), but contain relatively little dense gas as traced by CO(3–2) or CS(2–1) (Williams & Blitz 1998). The unbound clumps are “pressure confined” in that their internal kinetic pressure, which is primarily turbulent, is comparable to the mean pressure of the ambient GMC (Blitz 1991; Bertoldi & McKee 1992). Simulations suggest that these clumps are transient structures (see chapter by Ostriker et al.)

The nature of the interclump medium remains unclear: Blitz & Stark (1986) postulated that it is low density molecular gas, but this has been questioned by Schneider et al. (1996). Blitz (1990, 1993) showed that atomic envelopes around molecular clouds are quite common and that the atomic gas plausibly pervades the interclump medium. Williams et al. (1995) show that the HI associated with the molecular gas in the Rosette has about the same turbulent pressure, and suggest that it could serve as the confining medium.

Cloud, clump and core density profiles are reflections of the physics that shape their evolution, but the density profiles of clouds and clumps have received scant attention. For clouds, which often are quite amorphous without a clear central peak, the density profile is often difficult to define observationally. For clumps, Williams et al. (1995) showed that surface density profiles of pressure bound, gravitationally bound, and star-forming clumps all have similar power law indices close to 1. Formally, the fits range from -0.8 to -1.2, but these differences do not appear to be significant. For a spherical cloud of infinite extent,  $\Sigma(r) \propto r^{-1}$  implies  $\rho(r) \propto r^{-2}$ , suggesting that the (turbulent) pressure support is spatially constant. However, McLaughlin & Pudritz (1996) argued that for finite spheres, the volume density distribution can be considerably flatter than that inferred for infinite clumps. Density distributions inferred from observations also require consideration of beam-convolution effects. It is nevertheless astonishing that both strongly self-gravitating clumps and those bound by external pressure have such similar, perhaps identical density distributions. Why this should be so is unclear.

## E. Fractal Structures

An alternate description of the ISM is based on fractals. High spatial dynamic range observations of molecular clouds, whether by millimeter spectroscopy (e.g., Falgarone et al. 1998), IRAS (Bazell & Désert 1988), or using the Hubble Space Telescope (e.g., O’Dell & Wong 1996; Hester et al. 1996) show exceedingly complex patterns that appear to defy a simple description in terms of clouds, clumps and cores; Scalo (1990) has argued that such loaded names arose from lower dynamic range observations and a general human tendency to categorize continuous forms into discrete units.

As we have discussed above, it seems that however one analyzes

a molecular cloud dataset, one finds self-similar structures. Moreover, the highly supersonic linewidths that are observed in molecular clouds probably imply turbulent motions (see discussion in Falgarone & Phillips 1990), for which one would naturally expect a fractal structure (Mandelbrot 1982).

The fractal dimension of a cloud boundary,  $D$ , can be determined from the perimeter-area relation of a map,  $P \propto A^{D/2}$ . Many studies of the molecular ISM find a similar dimension,  $D \simeq 1.4$  (Falgarone et al. 1991 and references therein). In the absence of noise,  $D > 1$  demonstrates that cloud boundaries are fractal. That  $D$  is invariant from cloud to cloud (star-forming or quiescent, gravitationally bound or not) is perhaps related to the similarity in the mass spectrum index in many different molecular clouds (Kramer et al. 1998a; Heithausen et al. 1998). Fractal models have been used to explain both the observed mass spectrum of structures (Elmegreen & Falgarone 1996) and the stellar IMF (Elmegreen 1997b).

Probability density functions (PDFs) may be used to describe the distribution of physical quantities (such as density and velocity) in a region of space without resorting to concepts of discrete objects such as clouds, clumps and cores. The density PDF is readily determined from simulations, and can be semi-analytically modeled (Vazquez-Semadeni 1998) but is very difficult to determine from observations because projection and excitation effects result in maps of column density integrated over a limited range of volume density. We discuss column density PDFs in §III.F.

Velocities, albeit also projected, can be much more easily measured. Falgarone & Phillips (1990) show that the PDF of the velocity field can be determined from high signal-to-noise observations of a single line profile. The low-level, broad line wings that are observed in non-star forming regions show that the probability of rare, high-velocity motions in the gas are greater than predicted by a Normal (gaussian) probability distribution. This *intermittent* behavior is expected in a turbulent medium, and their detailed analysis shows that the deviations from the predictions for Kolmogorov turbulence are small despite the fact that the basic assumptions of Kolmogorov turbulence, such as incompressibility and  $B = 0$ , are not satisfied. Miesch & Scalo (1995) calculate velocity centroid PDFs from  $^{13}\text{CO}$  observations of star-forming regions and also report non-gaussian behaviour. Lis et al. (1996) compare their results with a similar analysis applied to simulations of compressible turbulence; such work may be a promising avenue for exploring the role of turbulence in molecular clouds.

A key project at the IRAM 30 m telescope has been the investigation of the small scale structure in pre-star forming regions (Falgarone et al. 1998). Their study of many high resolution, high spatial dynamic range maps in a number of different tracers and transitions

shows that the line core emission has a rather smooth and extended spatial distribution, but the line wing emission has a more filamentary distribution. These filaments also show very large local velocity gradients,  $\gtrsim 10 \text{ km s}^{-1} \text{ pc}^{-1}$ , and have the greatest amount of small scale structure.

Falgarone et al. also address a long standing problem concerning the extreme smoothness of observed line profiles. Isotopic ratios indicate that CO lines, especially at line center, are very optically thick, yet line profiles are generally neither flat topped nor self-reversed. Moreover, line profiles do not break up into separate components at high angular and spectral resolution. This has traditionally presented a problem for the clump-based picture of molecular clouds (Martin, Sanders, & Hills 1984). Falgarone et al. interpret their results in terms of a macroturbulent model: emission arises from a large number of cells with size  $\lesssim 200 \text{ AU}$  and densities ranging from  $n_{\text{H}_2} \sim 10^3 \text{ cm}^{-3}$  for line-wing emission, to  $n_{\text{H}_2} \sim 10^5 \text{ cm}^{-3}$  for line-core emission. They find that an anti-correlation between linewidth and intensity and speculate that as the turbulent motions dissipate, there is increased radiative coupling between cells. Macroturbulent models have also been explored by Wolfire, Hollenbach, & Tielens (1993) who include the effects of photodissociation, and Tauber (1996) who includes an interclump medium but finds no evidence for small scale structures ( $\lesssim 0.5 \text{ pc}$ ) in Orion A.

## F. Departures from self-similarity

The universal self-similarity that is observed in all types of cloud, over a wide range in mass and star forming activity is remarkable, but a consequence of this universality is that it does not differentiate between clouds with different rates of star formation (or those that are not forming stars at all) and therefore it cannot be expected to explain the detailed processes by which a star forms. Star formation must be preceded by a departure from structural self-similarity.

An upper limit to the range over which self-similar scaling laws apply is set by the generalization of the Bonnor-Ebert mass to non-thermal linewidths. From an analysis of the clumps in Ophiuchus, Orion B, the Rosette, and Cep OB 3, Bertoldi & McKee (1992) found that  $M_{\text{BE}} = 1.18\sigma^4/(G^3P)^{1/2}$  is about constant for all the pressure-confined clouds in each GMC. Here,  $\sigma$  is the total (thermal + non-thermal) velocity dispersion, For all but Cep OB 3, for which the data are of low resolution, star formation was confined to clumps with  $M \gtrsim M_{\text{BE}}$ , and essentially all the clumps with  $M > M_{\text{BE}}$  are forming stars. The maximum mass of a clump in these clouds was in the range  $(1 - 10)M_{\text{BE}}$  (for Cep OB 3, this statement applies only to the limited part of the cloud for which data were available).

On the small scale, there have long been suggestions that the thermal Bonnor-Ebert mass gives a scale that determines the characteristic

mass of stars (Larson 1985). In order to determine whether such a scale is important in molecular clouds, Blitz & Williams (1997) examined how the structural properties of a large scale, high resolution  $^{13}\text{CO}$  map of the Taurus molecular cloud obtained by Mizuno et al. (1995) varied as the resolution was degraded by an order of magnitude. In their work, they use the temperature histogram of the dataset to compare the cloud properties as a function of resolution. This is the most basic statistic and requires minimal interpretation of the data. In Figure 3 we show the column density PDF, which is proportional to the integrated intensity histogram for optically thin emission, for this Taurus dataset at two resolutions and four other  $^{13}\text{CO}$  maps of molecular clouds.

To compare the different cloud PDFs, Figure 3 shows column densities that have been normalized by the peak,  $N_{\text{peak}}$ , of each map. Each PDF has also been truncated at  $N/N_{\text{peak}} \simeq 0.15 - 0.25$  to show only those points with high signal-to-noise. Within the Poisson errors (not shown for clarity), the PDFs of the different clouds are all the same, except for the higher resolution Taurus PDF for which there is a lower relative probability of having lines of sight with  $N/N_{\text{peak}} \gtrsim 0.7$ . The low intensities of the  $^{13}\text{CO}$  emission imply that the optical depth is small along all lines of sight in the map, and is not responsible for this effect. Rather, from examination of the integrated intensity maps, Blitz & Williams (1997) show that this is due to a steepening of the column density profiles at small size scales (see also Abergel et al. 1994).

There are two immediate implications from Figure 3. First, the common exponential shape for the column density PDF is another manifestation of the self similar nature of cloud structure. It is a simple quantity to calculate and may provide a quick and useful test of the fidelity of cloud simulations.

Second, since the behavior of the Taurus dataset changes as it is smoothed, it cannot be described by a single fractal dimension over all scales represented in the map (see Williams 1998 for a demonstration that the intensity histogram of a fractal cloud is resolution invariant as one would expect). There is other evidence for departures from self-similarity at similar size scales. Goodman et al. (1998) examine in detail the nature of the size-linewidth relation in dense cores as linewidths approach a constant, slightly greater than thermal, value in a central “coherent” region  $\sim 0.1$  pc diameter (Myers 1983). Also, Larson (1995) finds that the two-point angular correlation function of T Tauri stars in Taurus departs from a single power law at a size scale of 0.04 pc (see also Simon 1997).

For gas of density  $n_{\text{H}_2} \sim 10^3 \text{ cm}^{-3}$ , these size scales correspond to masses of order  $\sim 1 M_{\odot}$ , close to the thermal Bonnor-Ebert mass at a temperature  $T = 10$  K. It must be emphasized that the above evidence for characteristic scales comes from studies of gravitationally

bound, star forming regions: self-similarity in unbound clouds continues to much smaller scales. Figure 3 shows that the column density PDF of the unbound, high latitude cloud MBM12 is identical, at a resolution of 0.03 pc, to the other lower resolution PDFs of star forming GMCs. Similarly, the mass spectra of other high latitude clouds follow power laws,  $dN/d\ln M \propto M^{-x}$  with  $x \simeq 0.6 - 0.8$ , down to extremely low masses,  $M \simeq 10^{-4} M_{\odot}$  (Kramer et al. 1998a; Heithausen et al. 1998). It appears to be the action of gravity that creates the observed departures from self-similarity.

#### IV. THE CONNECTION BETWEEN CLOUD STRUCTURE AND STAR FORMATION

##### A. Star-forming clumps

Star-forming clumps are bound regions in a molecular cloud that form stellar clusters. Since most stars form in clusters, questions of star formation efficiency and rate are tied into the efficiency and rate of formation of star-forming clumps, and the IMF is related to the fragmentation of such clumps into individual star forming cores.

The median column density of molecular gas in the outer Galaxy CO survey by Heyer et al. (1998) is only  $N(\text{H}_2) \simeq 2 \times 10^{21} \text{ cm}^{-2}$ , and most of the mass of a molecular cloud is contained within the low column density lines of sight,  $A_V \lesssim 2$  (Carpenter et al. 1995a; Heyer et al. 1996). Such gas is ionized predominantly by the interstellar far ultraviolet radiation field ( $h\nu < 13.6 \text{ eV}$ ). McKee (1989) showed that this is true throughout the Galaxy: most molecular gas is photoionized and therefore has a higher level of ionization than that due to cosmic rays alone. Since the rate of low-mass star formation may be governed by ambipolar diffusion, which in turn is determined by the ionization (e.g., Shu et al. 1987), low-mass star formation is “photoionization-regulated”: most stars form in regions shielded from photoionization by column densities of dust corresponding to  $A_V \gtrsim 3 - 4$ . This idea has been applied to the formation of star clusters by Bertoldi & McKee (1996). It naturally accounts for the low average rate of star formation in the Galaxy, since only about 10% of the mass of a typical GMC is sufficiently shielded to have active star formation, and the ambipolar diffusion timescale is about 10 times the free fall time. Observations of the ISM in the low metallicity Magellanic Clouds have verified the prediction that molecular clouds have about the same dust column densities, and therefore higher gas column densities, as Galactic molecular clouds (Pak et al. 1998). Li, Evans, & Lada (1997) have tested photoionization-regulated star formation by searching for evidence of recent star formation in low extinction regions of L1630; they found no evidence for such star formation. On the other hand, Strom et al.

(1993) did find evidence for distributed star formation in L1641; possible reasons for the discrepancy are discussed by Li et al. In addition, Nakano (1998) has questioned whether ambipolar diffusion plays any important role in low mass star formation. He has correctly pointed out that cores are magnetically supercritical, so that ambipolar diffusion is unimportant there, but he has not addressed the issue of whether ambipolar diffusion was important prior to the formation of the cores. An observational determination of the role of ambipolar diffusion in low mass star formation remains a challenge for the future.

## B. Cores

The core that forms an individual star (or multiple stellar system) is the final stage of cloud fragmentation. Cores have typical average densities  $n_{\text{H}_2} \sim 10^5 \text{ cm}^{-3}$  and can be observed in high excitation lines or transitions of molecules with large dipole moments (Benson & Myers 1989), or via dust continuum emission at millimeter and sub-millimeter wavelengths (Kramer et al. 1998b).

Because of their high densities, the surface filling fraction of cores is low, even in cluster forming environments. Therefore searches for cores have generally followed signs of star formation activity, e.g. IRAS emission, outflows, etc. and there have been few unbiased searches (e.g. Myers & Benson 1983). However, increases in instrument speed have now made it possible to survey millimeter continuum emission over relatively large areas of the sky. There have been two very recent results in this regard, the first by Motte, André, & Neri (1998) at 1.3 mm using the array bolometer on the IRAM 30 m telescope, and the second by Testi & Sargent (1998) at 3 mm using the OVRO interferometer.

Motte et al. (1998) mapped the  $\rho$  Ophiuchus cloud, the closest rich cluster forming region (see chapter by André et al.) and Testi & Sargent (1998) mapped the Serpens molecular cloud, a more distant, but more massive and somewhat richer star forming region (Figure 4). In each case, the large scale, high resolution observations reveal a large number of embedded young protostars and also starless, dense condensations. Both studies find that the mass spectrum of the cores is significantly steeper,  $x > 1.1$  (where  $dN/d \ln M \propto M^{-x}$ ) than clump mass spectra,  $x \simeq 0.6 - 0.8$ . The core mass spectra resemble the slope,  $x = 1.35$ , of the stellar (Salpeter) IMF which suggests a very direct link between cloud structure and star formation. However, it has not yet been shown that these starless cores are self-gravitating, which is an important step in establishing the link.

## C. The origin of the IMF

The spectrum, lifetime, and end state of a star are primarily determined by its mass. Consequently, the problem of understanding how the mass of a star is determined during its formation, and the origin of



the IMF, has a very wide application in many fields from galaxy evolution to the habitability of extrasolar planets. The form of the IMF is typically assumed to be invariant, but since it is directly measurable only locally, knowing how it comes about can help us predict how it might vary under different astrophysical environments.

Observations and theories of the IMF are discussed in detail in the chapter by Adams et al., but here we briefly note the connection between the work described in this chapter and the IMF. Many explanations for the form of the IMF use as their starting point the mass spectrum of clouds and clumps as revealed by molecular line emission,  $dN/d\ln M \propto M^{-x}$  with  $x \simeq 0.5$ . Most such structures, however, are not forming stars: the majority of stars form in clusters in a few of the most massive clumps in a cloud. An understanding of the origin of the IMF can only come about with a more complete picture of the formation of star-forming clumps and the fragmentation of these clumps down to individual star forming cores. The unbiased continuum surveys by Motte et al. (1998) and Testi & Sargent (1998) are an important step in this direction. As high resolution studies of individual cores in cluster environments become more commonplace, the relationship between stellar mass and core mass can be determined. If the core mass spectrum is indeed similar to the stellar IMF, then the fraction of the mass of a core that goes into a star (the star formation efficiency of the core) is approximately independent of mass and the stellar IMF is determined principally by the cloud fragmentation processes. By measuring the core mass spectrum in different clusters in a variety of different molecular clouds, the influence of the large scale structure and environment on the IMF can be quantified.

## V. SUMMARY

The study of the structure of molecular clouds is inextricably linked to the formation of stars. In the outer Galaxy the molecular gas is confined to spiral arms. The inner Galaxy also shows confinement of the molecular gas to the spiral arms, but there is some evidence for interarm molecular gas as well. The observed star formation rate and efficiency in the Galaxy may be the result of only about 10% of the molecular ISM being shielded from the interstellar UV radiation field to an extent that matter can drift through the magnetic field lines and condense into star forming cores on timescales  $\sim 10$  Myr.

Molecular clouds, in the outer Galaxy at least, probably result from the compression of atomic gas entering a spiral arm. Thus, the density inhomogeneities in clouds may simply reflect the initial non-uniform conditions of the atomic ISM and need not be related to star formation. At moderate densities,  $n_{\text{H}_2} \lesssim 10^3 \text{ cm}^{-3}$ , cloud structures are self-similar up to a scale set by self-gravity and clump mass-spectra

have similar power law indices independent of the star-forming nature of the cloud.

As linewidths approach their thermal value, structures depart from the same self-similar description. This departure may mark the boundary between cloud evolution and star formation. Clusters of individual star forming cores, with a mass spectrum that approaches the Salpeter IMF, are observed in the  $\rho$  Ophiuchus and Serpens clouds. In the coming years, we can expect there to be increased observational and theoretical effort to understand the structure, dynamics, and distribution of these cores in a variety of star forming environments which should lead to a better understanding of the relationship between the structure and evolution of molecular clouds and the initial mass function of stars.

We enjoyed many informative discussions with both Edith Falgarone and Dick Crutcher, and we thank them also for a thorough reading of the manuscript. We are grateful to Mark Heyer for providing figure 1 and for a series of interesting conversations over the last several years. Finally, thanks to Leonardo Testi for figure 4 in advance of publication.

## REFERENCES

- Abergel, A., Boulanger, F., Mizuno, A., & Fukui, Y. 1994. Comparative analysis of the far-infrared and (13)CO ( $J = 0-1$ ) emissions of the Taurus complex. *Astrophys. J. Lett.* 423:L59–L62.
- Adams, F.C. 1992. A topological/geometrical approach to the study of astrophysical maps. *Astrophys. J.* 387:572–590.
- Bally, J., Stark, A.A., Wilson, R.W., & Langer, W.D. 1987. Filamentary structure in the Orion molecular cloud. *Astrophys. J. Lett.* 312:L45–L49.
- Bazell, D., & Désert, F.X. 1988. Fractal structure of interstellar cirrus. *Astrophys. J.* 333:353–358.
- Benson, P.J., & Myers, P.C. 1989. A survey for dense cores in dark clouds. *Astrophys. J. Suppl.* 71:89–108.
- Bertoldi, F., & McKee, C.F. 1992. Pressure-confined clumps in magnetized molecular clouds. *Astrophys. J.* 395:140–157.
- Bertoldi, F., & McKee, C.F. 1996. Self-regulated star formation in molecular clouds. In *Amazing Light, A Volume Dedicated to Charles Hard Townes on His 80th Birthday*, ed. R.Y. Chiao (New York: Springer), pp. 41–44.
- Blitz, L. 1990. The Evolution of Galactic Giant Molecular Clouds. In *The Evolution of the Interstellar Medium*, ed. L. Blitz, (ASP Press: San Francisco), pp.273–289.
- Blitz, L. 1991. Star Forming Giant Molecular Clouds. In *The Physics of Star Formation and Early Stellar Evolution*, ed. C. J. Lada & N. D. Kylafis (Dordrecht: Kluwer), pp 3-33.
- Blitz, L. 1993. Giant molecular clouds. In *Protostars and Planets III*, eds. E.H. Levy and J.I. Lunine, (Tucson: Univ. of Arizona Press), pp. 125–161.
- Blitz, L. Magnani, L. and Mundy, L. 1984. High-Latitude Molecular Clouds. *Astrophys. J. Lett.* 282:L9–L12.
- Blitz, L., & Shu, F.H. 1980. The origin and lifetime of giant molecular cloud complexes. *Astrophys. J.* 238:148–157.
- Blitz, L., & Stark, A.A. 1986. Detection of clump and interclump gas in the Rosette molecular cloud complex. *Astrophys. J. Lett.* 300:L89–L93.
- Blitz, L., & Thaddeus, P. 1980. Giant molecular complexes and OB associations. I: The Rosette Molecular Complex. *Astrophys. J.* 241:676–696.
- Blitz, L., & Williams, J.P. 1997. Molecular clouds are not fractal: A

- characteristic size scale in Taurus. *Astrophys. J. Lett.* 488:L145–L149.
- Bonnell, I.A., Bate, M.R., Clarke, C.J., & Pringle, J.E. 1997. Accretion and the stellar mass spectrum in small clusters. *MNRAS* 285:201–208.
- Boulares, A., & Cox, D.P. 1990. Galactic hydrostatic equilibrium with magnetic tension and cosmic-ray diffusion. *Astrophys. J.* 365:544–558.
- Carpenter, J.M., Snell, R.L., & Schloerb, F.P. 1995a. Anatomy of the Gemini OB1 molecular cloud complex. *Astrophys. J.* 445:246–268.
- Carpenter, J.M., Snell, R.L., & Schloerb, F.P. 1995b. Star formation in the Gemini OB1 molecular cloud complex. *Astrophys. J.* 450:201–216.
- Clemens, D.P., & Barvainis, R. 1988. A catalog of small, optically selected molecular clouds: Optical, infrared, and millimeter properties *Astrophys. J. Suppl.* 68:257–286.
- Cohen, R.S., Cong, H.-I., Dame, T.M., & Thaddeus, P. 1980, Molecular Clouds and Galactic Spiral Structure. *Astrophys. J. Lett.* 239:L53–L56.
- Cox, P., Deharveng, L. & Leene, A. 1990. IRAS observations of the Rosette nebula complex. *Astron. Astrophys.* 230:181–192.
- Crutcher, R.M. 1999. Magnetic fields in molecular clouds—observations confront theory. *Astrophys. J.*, submitted.
- Crutcher, R.M., Mouschovias, T.M., Troland, T.H., & Ciolek, G.E. 1994. Structure and evolution of magnetically supported molecular clouds: Evidence for ambipolar diffusion in the Barnard 1 cloud. *Astrophys. J.* 427:839–847.
- Dame, T.M. et al. 1987. A composite CO survey of the entire Milky Way. *Astrophys. J.* 322:706–720.
- Dame, T.M., Elmegreen, B.G., Cohen, R.S., & Thaddeus, P. 1986. The largest molecular cloud complexes in the first galactic quadrant. *Astrophys. J.* 305:892–908.
- Digel, S.W., Lyder, D.A., Philbrick, A.J., Puche, D., & Thaddeus, P. 1996. A Large-Scale CO Survey toward W3, W4, and W5. *Astrophys. J.* 458:561–575.
- Elmegreen, B.G. 1997a. Intercloud structure in a turbulent fractal interstellar medium. *Astrophys. J.* 477:196–203.
- Elmegreen, B.G. 1997b. The initial stellar mass function from random sampling in a Turbulent Fractal Cloud. *Astrophys. J.* 486:944–954.
- Elmegreen, B.G. 1985. Molecular Clouds and Star formation: An Overview In *Protostars and Planets II*, eds. D.C. Black & M.S. Matthews, (Tucson: Univ. of Arizona Press), pp. 97–161.
- Elmegreen, B.G. 1993a. Formation of interstellar clouds and structure In *Protostars and Planets III*, eds. E.H. Levy and J.I. Lunine, (Tucson: Univ. of Arizona Press), pp. 97–161.

- Elmegreen, B.G. 1993b. The H to H<sub>2</sub> transition in galaxies: Totally molecular galaxies. *Astrophys. J.* 411:170–177.
- Elmegreen, B.G., & Lada, C.J. 1977. Sequential formation of subgroups in OB associations. *Astrophys. J.* 214:725–741.
- Elmegreen, B.G., & Falgarone, E. 1996. A fractal origin for the mass spectrum of interstellar clouds. *Astrophys. J.* 471:816–821.
- Falgarone, E., Panis, J.-F., Heithausen, A., Pérault, M., Stutzki, J., Puget, J.-L., & Bensch, F. 1998. The IRAM key-project: Small-scale structure of pre-star-forming regions. I. Observational results. *Astron. Astrophys.* 331:669–696.
- Falgarone, E., & Phillips, T.G. 1990. A signature of the intermittency of interstellar turbulence: The wings of molecular line profiles. *Astrophys. J.* 359:344–354.
- Falgarone, E., Phillips, T.G., & Walker C.K. 1991. The edges of molecular clouds: Fractal boundaries and density structure. *Astrophys. J.* 378:186–201.
- Fiege, J.D., & Pudritz, R.E. 1998. Helical Fields and Filamentary Molecular Clouds. *Mon. Not. Roy. Astron. Soc.* submitted (astro-ph/9901096).
- Goodman, A.A., Barranco, J.A., Wilner, D.J., & Heyer, M.H. 1998. Coherence in dense cores. II. The transition to coherence. *Astrophys. J.* 504:223–246.
- Heyer, M.H., Brunt, C., Snell, R. L., Howe, J. E., Schloerb, F. P., & Carpenter, J. M. 1998. The Five College Radio Astronomy Observatory CO survey of the outer Galaxy. *Astrophys. J. Suppl.* 115:241–258.
- Heyer, M.H., Carpenter, J.M., & Ladd, E.F. 1996. Giant molecular cloud complexes with optical HII regions: <sup>12</sup>CO and <sup>13</sup>CO observations and global cloud properties. *Astrophys. J.* 463:630–641.
- Heyer, M.H., & Schloerb, F.P. 1997. Application of principal component analysis to large-scale spectral line imaging studies of the interstellar medium. *Astrophys. J.* 475:173–187.
- Heyer, M.H., & Terebey, S. 1998. The anatomy of the Perseus spiral arm: <sup>12</sup>CO and IRAS imaging observations of the W3–W4–W5 cloud complex. *Astrophys. J.* 502:265–277.
- Heithausen, A., Bensch, F., Stutzki, J., Falgarone, E., & Panis, J.-F. 1998. The IRAM key project: Small-scale structure of pre-star forming regions. Combined mass spectra and scaling laws. *Astron. Astrophys. Lett.* 331:L65–L68.
- Hester, J.J., et al. 1996. Hubble Space Telescope WFPC2 Imaging of M16: Photoevaporation and emerging young stellar objects. *Astron. J.* 111:2349–2360.
- Heiles, C. 1996. in *Polarimetry of the Interstellar Medium*, eds. W.G. Roberge and D.C.B. Whittet (ASP: San Francisco).
- Heiles, C., Goodman, A.A., McKee, C.F., & Zweibel, E.G. 1993. Mag-

- netic fields in star-forming regions: Observations. In *Protostars and Planets III*, eds. E.H. Levy and J.I. Lunine, (Tucson: Univ. of Arizona Press), pp. 279–326.
- Houllahan, P., & Scalo, J. 1992. Recognition and characterization of hierarchical interstellar structure. II: Structure tree statistics. *Astrophys. J.* 393:172–187.
- Jackson, J.D. 1975. *Classical Electrodynamics* (Wiley: New York)
- Kramer, C., Stutzki, J., Röhrig, R., Corneliussen, U. 1998a. Clump mass spectra of molecular clouds. *Astron. Astrophys.* 329:249–264.
- Kramer, C., Alves, J., Lada, C., Lada, E., Sievers, A., Ungerechts, H., & Walmsley, M. 1998b. The millimeter wavelength emissivity in IC5146. *Astron. Astrophys. Lett.* 329:L33–L36.
- Kuchar, T.A., & Bania, T.M. 1993. A high-resolution HI survey of the Rosette nebula. *Astrophys. J.* 414:664–671.
- Kutner, M.L., Tucker, K.D., Chin, G., & Thaddeus, P. 1977. The molecular complexes in Orion. *Astrophys. J.* 215:521–528.
- Lada, C.J., Lada, E.A., Clemens, D.P., & Bally, J. 1994. Dust extinction and molecular gas in the dark cloud IC5146. *Astrophys. J.* 429:694–709.
- Lada, E.A. Strom, K.M., & Myers, P.C. 1993. Environments of star formation: Relationship between molecular clouds, dense cores and young stars. In *Protostars and Planets III*, eds. E.H. Levy and J.I. Lunine, (Tucson: Univ. of Arizona Press), pp. 247–277.
- Langer, W.D., Wilson, R.W., Anderson, C.H. 1993. Hierarchical structure analysis of interstellar clouds using nonorthogonal wavelets. *Astrophys. J. Lett.* 408:L45–L48.
- Larson, R.B. 1995. Star formation in groups. *Mon. Not. Roy. Astron. Soc.* 272:213–220.
- Larson, R.B. 1985. Cloud fragmentation and stellar masses. *Mon. Not. Roy. Astron. Soc.* 214:379–398.
- Larson, R.B. 1981. Turbulence and star formation in molecular clouds. *Mon. Not. Roy. Astron. Soc.* 194:809–826.
- Li, W., Evans, N.J., & Lada, E.A. 1997. Looking for distributed star formation in L1630: A near-infrared (J, H, K) survey. *Astrophys. J.* 488:277–285.
- Lis, D.C., Pety, J., Phillips, T.G., & Falgarone, E. 1996. Statistical properties of line centroid velocities and centroid velocity increments in compressible turbulence. *Astrophys. J.* 463:623–629.
- Loinard, L., Dame, T.M., Koper, E., Lequeux, J., Thaddeus, P., & Young, J.S. 1996. Molecular spiral arms in M31. *Astrophys. J. Lett.* 469:L101–L104.
- Loren, R.B. 1989. The cobwebs of Ophiuchus. I: Strands of  $^{13}\text{CO}$  – The mass distribution. *Astrophys. J.* 338:902–924.
- Maddalena, R., & Thaddeus, P., 1985. A large, cold, and unusual molecular cloud in Monoceros. *Astrophys. J.* 294:231–237.

- Magnani, L., Caillault, J.-P., Buchalter, A., & Beichman, C.A. 1995. A search for T Tauri stars in high-latitude molecular clouds. II: The IRAS Faint Source Survey catalog. *Astrophys. J. Suppl.* 96:159–173.
- Mandelbrot, B.B. 1982. *The Fractal Geometry of Nature* (San Francisco: Freeman)
- Martin, H.M., Sanders, D.B., & Hills, R.E. 1984. CO emission from fragmentary molecular clouds: A model applied to observations of M17 SW. *Mon. Not. Roy. Astron. Soc.* 208:35–55.
- McLaughlin, D.E., and Pudritz, R.E. 1996. A Model for the Internal Structure of Molecular Cloud Cores. *Astrophys. J.* 469:194–208.
- McKee, C.F. 1989. Photoionization-regulated star formation and the structure of molecular clouds. *Astrophys. J.* 345:782–801.
- McKee, C.F., Zweibel, E.G., Goodman, A.A., & Heiles, C. 1993. Magnetic fields in star-forming regions: Theory. In *Protostars and Planets III*, eds. E.H. Levy and J.I. Lunine, (Tucson: Univ. of Arizona Press), pp. 327–366.
- Miesch, M.S., & Scalo, J.M. 1994. Statistical analysis of turbulence in molecular clouds. *Astrophys. J.* 429:645–671.
- Mizuno, A., Onishi, T., Yonekura, Y., Nagahama, T., Ogawa, H., & Fukui, Y. 1995. Overall distribution of dense molecular gas and star formation in the the Taurus cloud complex. *Astrophys. J. Lett.* 445:L161–L165.
- Moriarty-Schieven, G.H., Andersson, B.-G., & Wannier, P.G. 1997. The L1457 Molecular/Atomic cloud complex: HI and CO Maps. *Astrophys. J.* 475:642–660.
- Motte, F., André, Ph., & Neri, R. 1998. The initial conditions of star formation in the  $\rho$  Ophiuchi main cloud: wide-field millimeter continuum mapping. *Astron. Astrophys.* 336:150–172.
- Myers, P.C. 1983. Dense cores in dark clouds: III. Subsonic turbulence. *Astrophys. J.* 270:105–118.
- Myers, P.C., & Benson P.J. 1983. Dense cores in dark clouds. II: NH<sub>3</sub> observations and star formation. *Astrophys. J.* 266:309–320.
- Myers, P.C., & Goodman, A.A. 1988. Evidence for Magnetic and Virial Equilibrium in Molecular Clouds. *Astrophys. J.* 326:L27–30
- Nagahama, T., Mizuno, A., Ogawa, H., & Fukui, Y. 1998. A spatially complete <sup>13</sup>CO  $J = 1 - 0$  survey of the Orion A cloud. *Astron. J.* 116:336–348.
- Nakano, T. 1998. Star formation in magnetic clouds. *Astrophys. J.* 494:587–604.
- Nakano, T., & Nakamura, T. 1978. Gravitational instability of magnetized gaseous disks. *Publ. Astron. Soc. Japan* 30:681–679.
- Normandeau, M., Taylor, A.R., & Dewdney, P.E. 1997. The Dominion Astrophysical Observatory Galactic plane survey pilot project: The W3/W4/W5/HB 3 region. *Astrophys. J. Suppl.* 108:279–299.

- O'Dell, C.R., & Wong, S.K. 1996. Hubble Space Telescope mapping of the Orion nebula. I. A survey of stars and compact objects. *Astron. J.* 111:846–855.
- Pak, S., Jaffe, D.T., van Dishoeck, E.F., Johansson, L.E.B., & Booth, R.S. 1998. Molecular cloud structure in the Magellanic Clouds: Effect of metallicity. *Astrophys. J.* 498:735–756.
- Patel, N., Goldsmith, P.F., Snell, R.L., Hezel, T., & Taoling, X. 1995. The large-scale structure, kinematics, and evolution of IC 1396. *Astrophys. J.* 447:721–741.
- Sanders, D.B., Clemens, D.P., Scoville, N.Z., & Solomon, P.M. 1985. Massachusetts-Stony Brook Galactic plane CO survey. I: (b,V) maps of the first Galactic quadrant. *Astrophys. J. Suppl.* 60:1–303.
- Sanders, D.B., Scoville, N.Z., & Solomon, P.M. 1985. Giant Molecular Clouds in the Galaxy II: Characteristics of Discrete Features. *Astrophys. J.* 289:373–387.
- Scalo, J. 1990. Perception of interstellar structure: Facing complexity. In *Physical Processes in Fragmentation and Star Formation*, eds. R. Capuzzo-Dolcetta et al. (Dordrecht: Kluwer) pp. 151–171.
- Schneider, N., Stutzki, J., Winnewisser, G., & Blitz, L. 1996. The nature of the molecular line wing emission in the Rosette molecular complex. *Astrophys. J. Lett.* 468:L119–L122.
- Shu, F.H., Adams, F.C., and Lizano, S., 1987. Star formation in molecular clouds: Observation and theory. *Ann. Rev. Astron. Astrophys.* 25:23–81.
- Shu, F.H., & Li, Z.-Y. 1997. Magnetic forces in an isopedic disk. *Astrophys. J.* 475:251–259.
- Simon, M. 1997. Clustering of young stars in Taurus, Ophiuchus, and the Orion trapezium. *Astrophys. J. Lett.* 482:L81–L84.
- Solomon, P.M., & Rivolo, A.R. 1989. A face-on view of the first galactic quadrant in molecular clouds. *Astrophys. J.* 339:919–925.
- Strom, K.M., Strom, S.E., & Merrill, K.M. 1993. Infrared luminosity functions for the young stellar population associated with the L1641 molecular cloud. *Astrophys. J.* 412:233–253.
- Stutzki, J., Bensch, F., Heithausen, A., Ossenkopf, V., & Zielinsky, M. 1998. On the fractal structure of molecular clouds. *Astron. Astrophys.* 336:697–720.
- Stutzki, J., & Güsten, R., 1990. High spatial resolution isotopic CO and CS observations of M17 SW: The clumpy structure of the molecular cloud core. *Astrophys. J.* 356:513–533.
- Tauber, J.A. 1996. The smoothness of line profiles: a useful diagnostic of clump properties. *Astron. Astrophys.* 315:591–602.
- Testi, L., & Sargent, A.I. 1998. The OVRO 3 mm continuum survey for compact sources in the Serpens core. *Astrophys. J. Lett.* 508:L91–L94.



- Tomisaka, K. 1991. The equilibria and evolutions of magnetized, rotating, isothermal clouds. V: The effect of the toroidal field. *Astrophys. J.* 376:190–198.
- van Dishoeck, E.F., & Black, J.H. 1988. The photodissociation and chemistry of interstellar CO. *Astrophys. J.* 334:771–802.
- Vazquez-Semadeni, E. 1998. Turbulence as an organizing agent in the ISM. In *Interstellar Turbulence, Proceedings of the 2nd Guillermo Haro Conference*, eds. J. Franco and A. Carraminana, (Cambridge University Press), in press.
- Williams, J.P. 1998. The structure of molecular clouds: Are they fractal? In *Interstellar Turbulence, Proceedings of the 2nd Guillermo Haro Conference*, eds. J. Franco and A. Carraminana, (Cambridge University Press), in press.
- Williams, J.P., & Blitz, L. 1998. A multitransition CO and CS(2–1) comparison of a star-forming and a non-star-forming giant molecular cloud. *Astrophys. J.* 494:657–673.
- Williams, J.P., Blitz, L., & Stark, A.A. 1995. The density structure in the Rosette molecular cloud: Signposts of evolution. *Astrophys. J.* 451:252–274.
- Williams, J.P., de Geus, E.J., & Blitz, L. 1994. Determining structure in molecular clouds. *Astrophys. J.* 428:693–712.
- Williams, J.P., & Maddalena, R.J. 1996. A large photodissociation region around the cold, unusual cloud G216-2.5. *Astrophys. J.* 464:247–255.
- Williams, J.P., & McKee, C.F. 1997. The Galactic distribution of OB associations in molecular clouds. *Astrophys. J.* 476:166–183.
- Wiseman, J.J., & Adams, F.C. 1994. A quantitative analysis of IRAS maps of molecular clouds. *Astrophys. J.* 435:708–721.
- Wolfire, M.G., Hollenbach, D., & Tielens, A.G.G.M. 1993. CO(J=1–0) line emission from giant molecular clouds. *Astrophys. J.* 402:195–215.
- Wood, D.O.S., Myers, P.C., & Daugherty, D.A. 1994. IRAS images of nearby dark clouds. *Astrophys. J. Suppl.* 95:457–501.



## The Structure and Evolution of Molecular Clouds

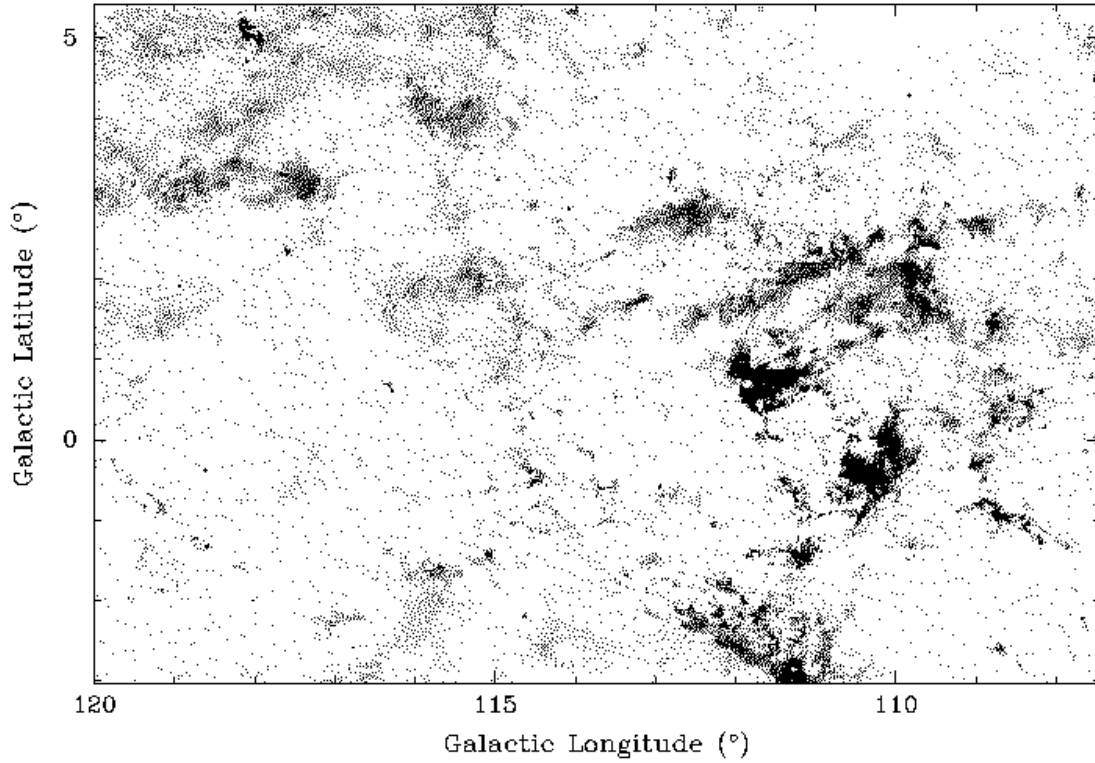


**Figure 1:** Velocity integrated CO emission in the outer Galaxy (from Heyer et al. 1998). This map, made with the 15 beam QUARRY receiver on the FCRAO telescope, contains over half a million spectra and shows a little less than 1/3 of their outer Galaxy survey. The grayscale ranges from 4 to 40 K km s<sup>-1</sup>. The high spatial dynamic range of this survey shows the large scale distribution of molecular gas in the ISM in exceptional detail.

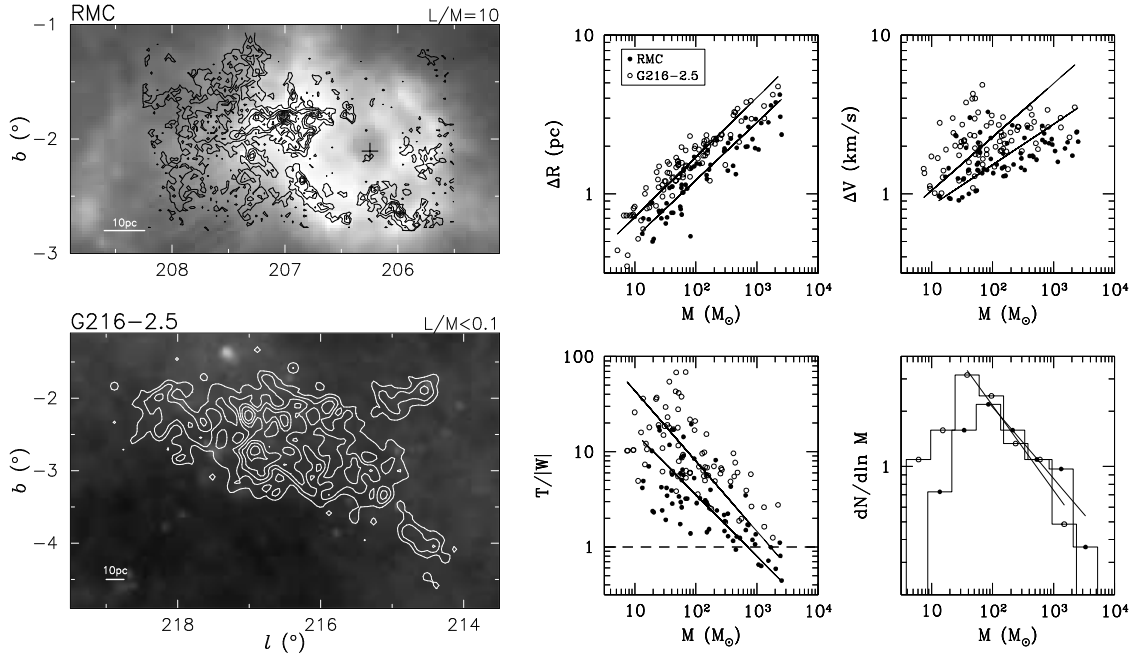


**Figure 2:** Structure in the Rosette and G216-2.5 molecular clouds. The two left panels show contours of velocity integrated CO emission (levels at  $15 \text{ K km s}^{-1}$  for the RMC,  $1.8 \text{ K km s}^{-1}$  for G216-2.5) overlaid on a grayscale image of the IRAS  $100 \mu\text{m}$  intensity ( $1.1$  to  $2.5 \text{ MJy sr}^{-1}$ , same for both clouds). The Rosette cloud is infrared bright, indicative of its high star formation rate, but G216-2.5 has a very low infrared luminosity due to a lack of star formation within it. The four rightmost panels show power law relations between clump mass and size, linewidth, energy balance (i.e. the ratio of kinetic energy,  $\mathcal{T} = 3M(\Delta v/2.355)^2/2$ , to gravitational potential energy, approximated as  $\mathcal{W} = -3GM^2/5R$ ), and number (i.e. clump mass spectrum) for the two clouds. The solid circles represent clumps in the RMC, and open circles represent clumps in G216-2.5. Each relationship has been fit by a power law: note that the power law exponent is approximately the same for the clumps in each cloud despite the large difference in star formation activity.

## The Structure and Evolution of Molecular Clouds

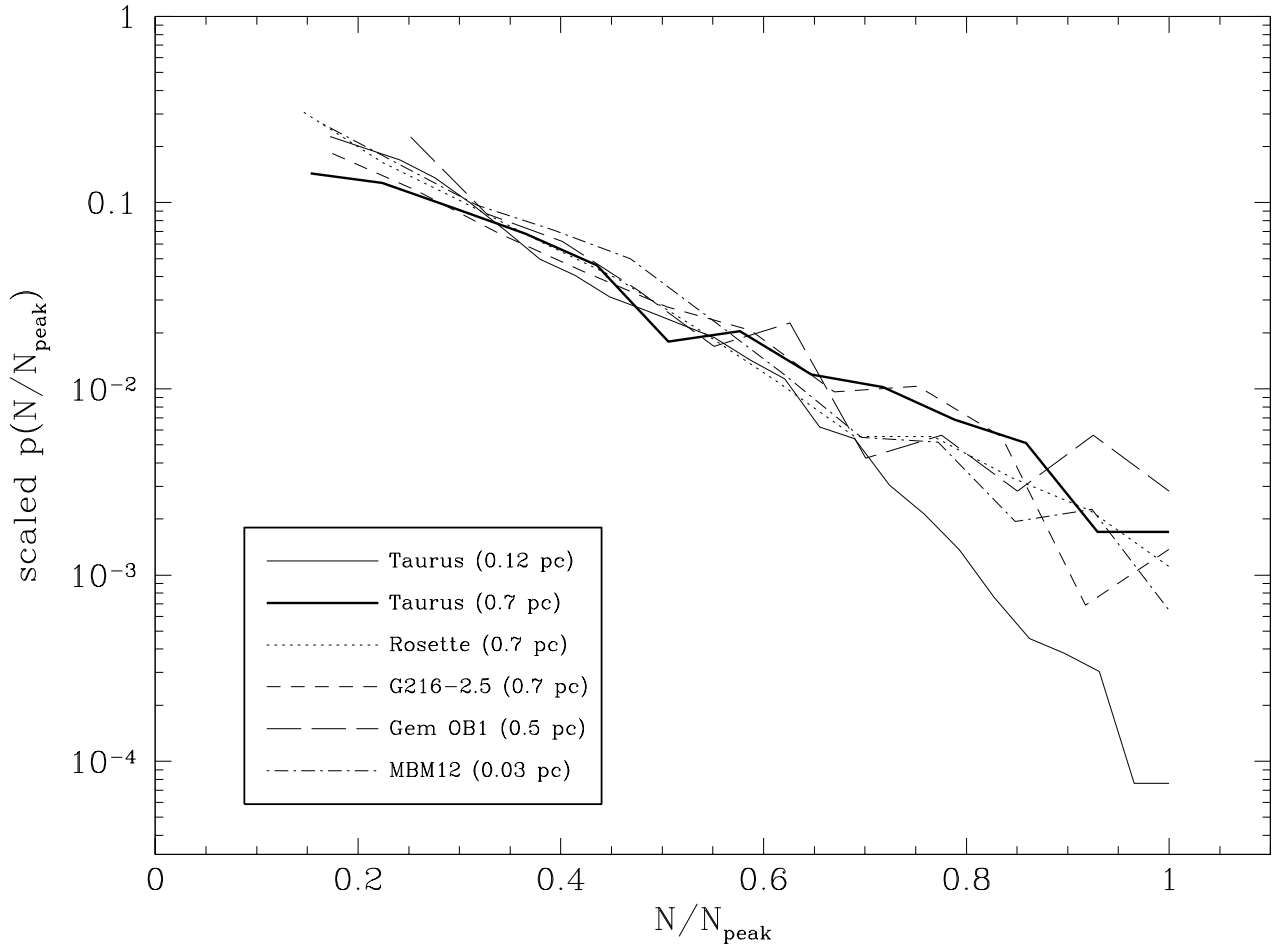


**Figure 3:** Column density PDF of  $^{13}\text{CO}$  emission in five molecular clouds. Column densities have been normalized by the peak value in each dataset and then binned. The fraction of data points in each bin is plotted as a function of normalized column density. The ordinate has been arbitrarily scaled so as to align the different curves at low column densities. Note the similarity between the different datasets, except for the high resolution Taurus map which has a lower fraction of data points with column densities within 70% of the peak.

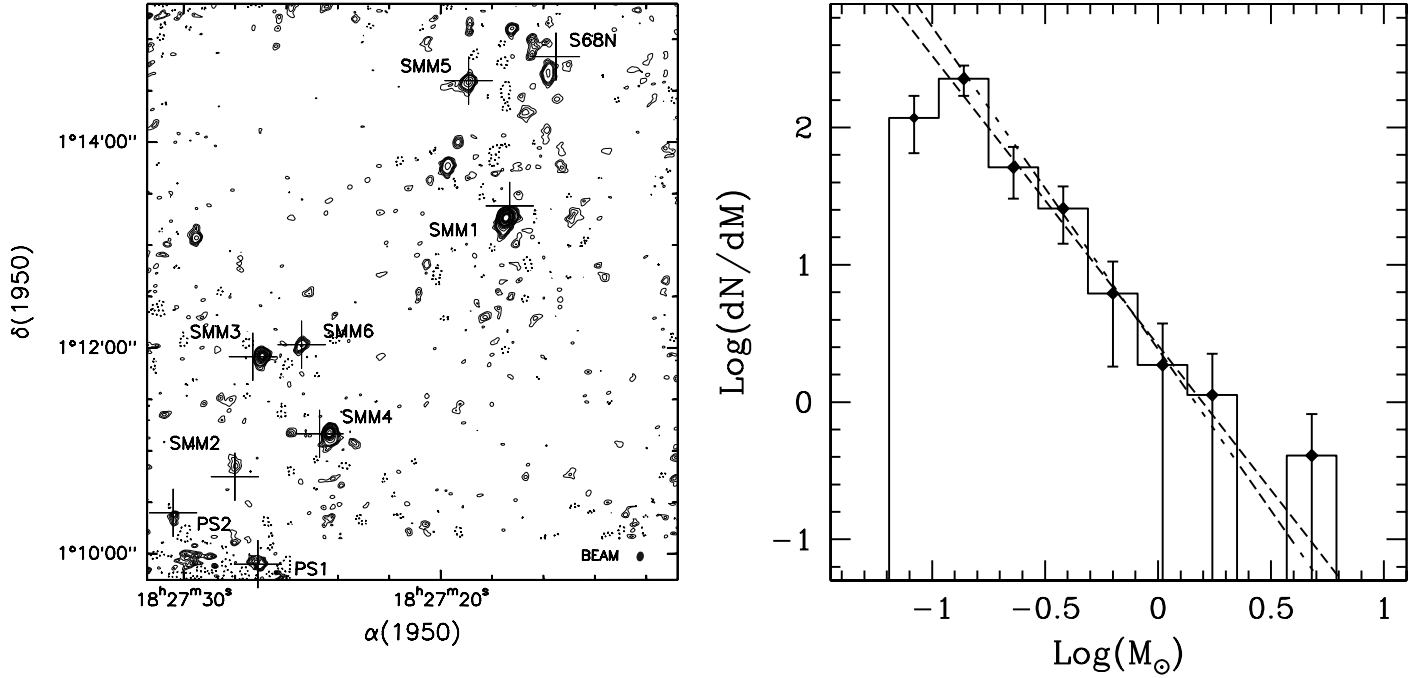


**Figure 4:** 3 m continuum emission in the Serpens molecular cloud (from Testi & Sargent 1998). This map is the result of a mosaic of 50 fields using the OVRO interferometer. The synthesized beam is  $5.7'' \times 4.3''$  (FWHM) and is indicated by the filled ellipse in the lower right corner. The noise level is  $\sigma = 0.9 \text{ mJy beam}^{-1}$  and contours begin and are in steps of  $3\sigma$ . A large number of sources, each a dense dust condensation, are visible. The previously known far-infrared and sub-millimeter sources are marked with crosses and labeled. The core mass spectrum has a slope  $dN/dM \propto M^{-2.1}$ , and more closely resembles the Salpeter IMF than the clump mass spectrum in molecular clouds.